Mounting of large lithium fluoride space-based optics

Todd Kvamme, Dario Trevias, RaShelle Simonson, Larry Sokolsky
Lockheed Martin Advanced Technology Center

ABSTRACT

Single crystal Lithium Fluoride has been base-lined as one of the optical materials for the Near Infra-Red Camera (NIRCam) on the James Webb Space Telescope (JWST). Optically, this material is outstanding for use in the near IR. Unfortunately, this material has poor mechanical properties, which make it very difficult for use in any appreciable size on cryogenic space based instruments. In addition to a dL/L from 300K to 30K of ~-0.48%, and a room temperature CTE of ~37ppm/K, the material deforms plastically under relatively small tensile loading. This paper will present a mount that has been proven via vibration and thermal-vacuum testing to successfully mount a large (70mm-94mm) Lithium Fluoride optic for application in space. An overview of Lithium Fluoride material properties and characteristics is given. A design limit load is determined for the material based on strength values from the literature as well as independent testing. The original design option is shown and the pros and cons discussed. The final mount design is then presented along with analysis results showing compliance to the limit load requirement. Finally, testing results are discussed showing survival of the optic in a space launch vibration environment as well as survival and performance during cool-down to the operational thermal environment of 30K.

Keywords: NIRCam, James Webb, Lithium Fluoride, cryogenic, mount, flexure

1. INTRODUCTION

The Near Infrared Camera (NIRCam) instrument for NASA's James Webb Space Telescope (JWST) is one of the four science instruments installed into the Integrated Science Instrument Module (ISIM) on JWST intended to conduct scientific observations over a five year mission lifetime. NIRCam's requirements include operation at 37 Kelvin to produce high resolution images in two wave bands encompassing the range from 0.6 microns to 5 microns. In addition NIRCam is used as a metrology instrument during the JWST observatory commissioning on orbit, during the initial and subsequent precision alignments of the observatory's multiple-segment 6.3 meter primary mirror. JWST is scheduled for launch and deployment in 2012.

This paper discusses the mounting design for the refractive optics in the NIRCam instrument.

2.0 REQUIREMENTS

Three optical materials were chosen by the NIRCam optics team to meet the optical performance criteria for the NIRCam instrument. They are Lithium Fluoride (LiF) , Barium Fluoride (BaF2) , and Zinc Selenide (ZnSe). The physical properties of these materials proved to be of primary importance and a driving factor in the design process. In addition to coping with these material properties, the NIRCam instrument will also need to survive a rather severe environmental change from launch to operation. JWST will be launched warm (~300K) but operate cold (~35K). The optical system must therefore survive a warm launch vibration environment, and then survive and perform on orbit after cooling nearly 265K. Optical system requirements are also stringent, with lens to lens alignments needing to be within +/- 50 microns of target values at operation.

3.0 MATERIAL CONSIDERATIONS – LITHIUM FLUORIDE

As mentioned above, the NIRCam program has chosen, as it's primary optical materials, LiF, BaF_2, and ZnSe. LiF is known to have the lowest mechanical strength of all these materials as well as other challenging properties, so it has been chosen as our baseline material for test and mount development. LiF is a cubic single crystal material. Aside from a room temperature coefficient of thermal expansion (CTE) of ~35ppm/K, a slight propensity to absorb water

(0.27g/100g water at 20ºC), and a very low apparent elastic limit in its commercially pure single crystal form (11Mpa), the one factor that makes LiF difficult to mount for space launch is its tendency toward plastic behavior at stresses well below its published apparent elastic limit. When a single crystal specimen is put under a relatively small amount of stress, dislocations within the crystal lattice will move, causing the material to deform plastically. This behavior can continue until the effects are visible at a macroscopic level, as can be seen in the post-test image taken of a four-point bend specimen in Figure 1.

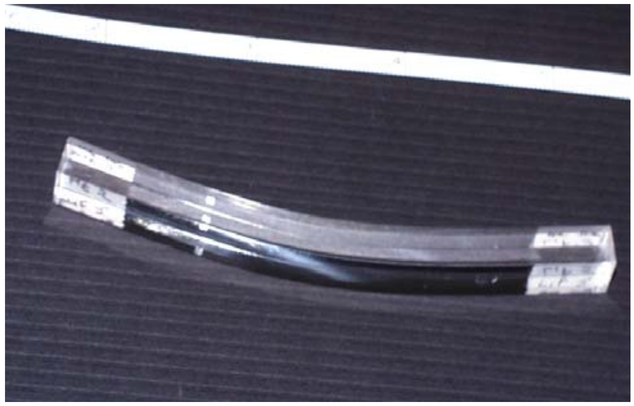

Figure 1 – LiF specimen (90mm X 8mm X 6mm) yielded after 4-point bend test

Why the material exhibits this behavior is a question outside the scope of this paper. A more appropriate question for this discussion is, "*When* (that is, at what stress level) does the material exhibit this behavior?" In order to answer this question it is important to realize that single crystals do not behave in the same manner as poly-crystalline materials. Often, their properties vary significantly in different directions of loading due to the structure of the crystal lattice. The crystallographic planes in the material which are least able to resist a shear force due to weak atomic interaction are called slip planes. In LiF, slip occurs in the {110} family of planes and along the <110> direction. Therefore, when a force is applied to this material, it is important to know how that force is resolved onto the slip planes. The *critical* resolved shear stress is the value at which the material will start to slip. (see reference 1) In an optical mount, we obviously want our resolved shear stress to remain below this value.

In addition to understanding the resolved critical shear stress in the mount, it is important to realize that with LiF, the surface quality of the optic will have a direct impact on the strength of the optic. In general, the better the polish of the surface, the stronger the material will be. Obtaining a high quality polish on a LiF optic can be challenging due to weak lattice interaction in the material (ref. 1). While this topic is also outside the scope of this paper, we can conclude that for purposes of strength, every surface, including radii and flats, should be polished in a LiF optic that will ultimately be launched into space.

For the purposes of our design, we have determined that 2MPa is the critical resolved shear stress for this material at 293K. A discussion of how this value was arrived at, as well as a more detailed discussion on the properties of LiF, can be found in reference 2. All surfaces on all LiF optics in NIRCam have also been polished to transparency. (see reference 3)

3.0 OPTO-MECHANICAL DESIGN AND ANALYSIS

Mechanical Design

The design for this mount is focused on limiting the stress induced on the optic during launch and on keeping the optic centered during cool-down and operation. Originally, a three-point flexure pad design was developed to accommodate the LiF optic. This mount basically consisted of two pads that held the optic radially while a third pad provided the radial pre-load. In between the metal pads and the optic was a low modulus, compliant material. (See figure 2). In the axial direction, a multi-finger flexure was employed to seat the optic into the cell. It also had the same low modulus material between it and the lens. This mount had several drawbacks however. The radial pads were originally intended to spread out the mounting load and accommodate radius change as the optic cooled. But it failed to do this, and the lack of radial compliance and a less than optimal pad design caused the optic to yield significantly during vibe.

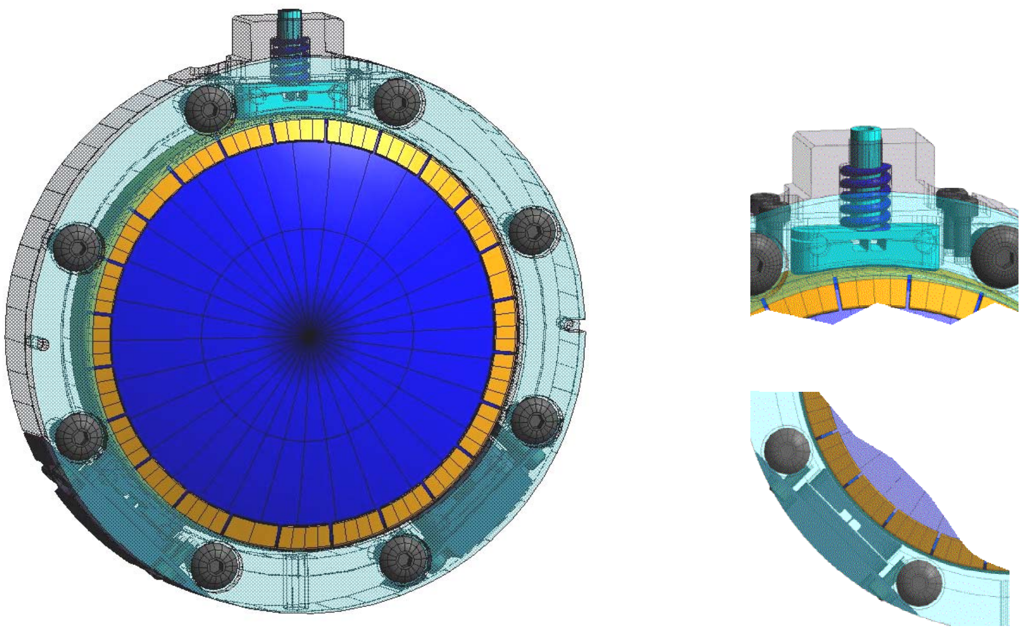

Figure 2 – Original 3 pad flexure design at left. At right, the spring loaded plunger and flexured pad (2places).

Many waves (measured at λ=633nm) of optical distortion were found at the two lower none spring loaded pads. (Figure 3) Even if this mount had worked, centration of the lens relative to the mount was going to be tricky. When cooled, the lens did not shrink relative to the center of the lens cell, rather it shrank about an axis that went through the two radial hard stops.   Accurate predictions of CTE in the system would be needed to guarantee that the lens would shrink into the proper place when cooled. Given the tight tolerance for optic position at operation, this was not going to be a viable method to address the requirements.

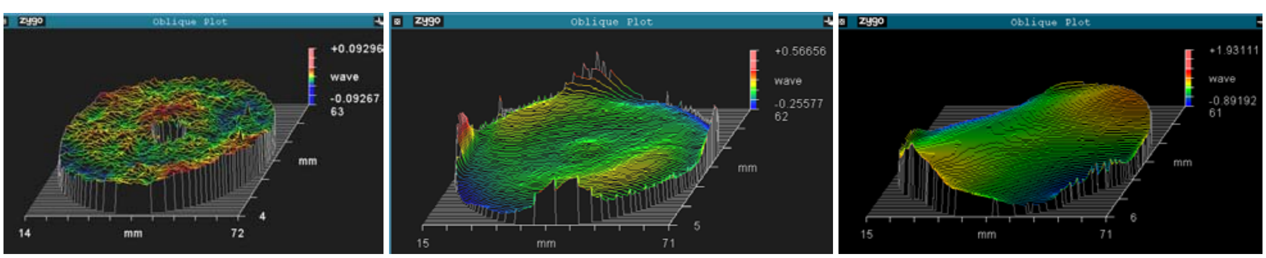

Figure 3 – In the left image is a ZYGO surface map of the LiF optic as received by the vendor. Total rms WFE = 0.012 waves at λ=633n; 0.186 wave P-V. The middle image shows the optic after having been mounted, and then removed from the mount. Clearly there is already distortion evident in the optic with rms WFE = 0.073 wav; 0.822 P-V. The right image shows the optic unmounted after vibration. Many waves of distortion at the radial mount points that were off-scale.

Once this design was discarded, a new design was developed that took the following requirements into account: 1) Low stress on the optic, 2) capable of being launched warm, 3) capable of surviving and staying aligned after a 265K decrease in temperature and 4) and a desire to keep the lens centered in the mount at all times. The result of this effort was a 12-pad circumferential flexure design. (Figure 4).

Figure 4 – The diamond flexure lens cell design and manufactured titanium lens cell hub

Each of the twelve flexures is shaped in the form of a diamond. The diamond flexures include a pad that interfaces the optic and is contoured to match the radius of that optic and shaped so as to avoid any punch load onto the optic. In order to spread out the load at each pad, a compliant, low modulus material is placed in between the metal flexure pads and the lens as was done in the original design. This prevents any metal to crystal contact, which could result in local deformation of the crystal. Each of the 12 radial pads is preloaded to allow appropriate limited motion during launch, but also keep the optic well centered. The pre-load must also be low enough to prevent the material from yielding during launch and cool-down, when mechanical and thermal stress will be at there highest. (See Mechanical Analysis section).

In the axial direction, the optic is loaded into the base of the lens cell via 12 flexures around the circumference of the lens. Each flexure has the same compliant, low modulus material below it that was used for the radial pads again with the intention of preventing metal to crystal contact. See figure 5.

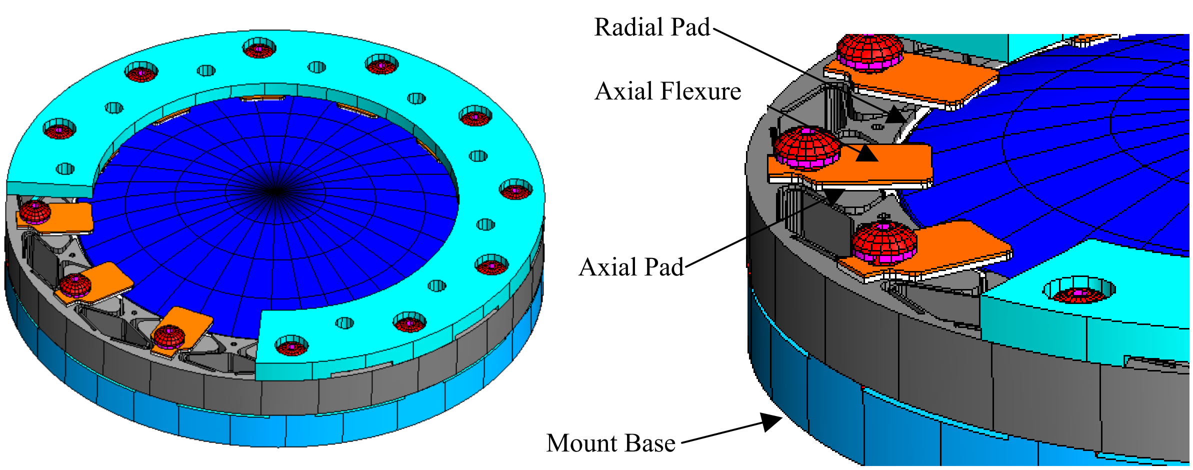

Figure 5- Lens cell cutaway and detail of axial and radial flexure and pads

Mechanical Analysis

Several questions need to be addressed in the mechanical analysis of this mount. The stress on the optic during launch is of primary importance as is the dynamic behavior of the mount. For the purposes of our analysis we have used values from the Goddard Environmental Verification Specification (GEVS) (ref. 4). The mount was designed to a 54 g static load value using the mass versus acceleration curve applicable to the JWST launch (see figure 6). In addition, the mount was checked against the effects of random vibration loading using an overall Qualification level vibration level of 14.1 g_{rms} from the GEVS (figure 7). The optic was therefore mounted in its cell with a calculated static preload in the radial and axial directions. The preload was determined from the load distribution on the radial pads under 54 G's inertial loading.

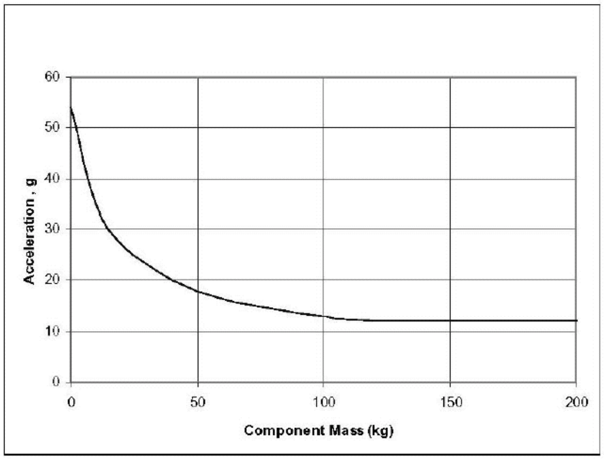

Figure 6 – Mass acceleration curve relevant to NIRCam

Frequency (Hz)	ASD Level (G^2/Hz)	
	Qualification	Acceptance
20	0.026	0.013
20-50	+6 dB/oct	+6 dB/oct
50-800	0.16	0.08
800-2000	-6 dB/oct	-6 dB/oct
2000	0.026	0.013
Overall	14.1 G_{rms}	10.0 G_{rms}

The acceleration spectral density level may be reduced for components weighing more than 22.7-kg (50 lb) according to:

	Weight in kg	Weight in lb	
dB reduction	= 10 log(W/22.7)	10 log(W/50)	
$ASD_{(50\text{-}800\ Hz)}$	= 0.16•(22.7/W)	0.16•(50/W)	for protoflight
$ASD_{(50\text{-}800\ Hz)}$	= 0.08•(22.7/W)	0.08•(50/W)	for acceptance

Where W = component weight.

The slopes shall be maintained at + and - 6dB/oct for components weighing up to 59-kg (130-lb). Above that weight, the slopes shall be adjusted to maintain an ASD level of 0.01 G^2/Hz at 20 and 2000 Hz.

For components weighing over 182-kg (400-lb), the test specification will be maintained at the level for 182-kg (400 pounds).

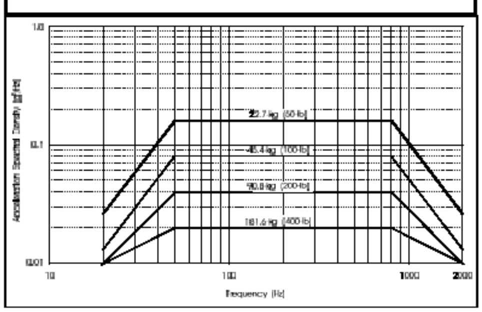

Figure 7 – Vibration test spectrum from GEVS (ref.

Only 5 of 12 radial flexures were assumed to carry the load. This results in a 16.24 N force at one pad which in turn causes a 0.50 MPa stress on the optic (See figure 8). Given that we have oriented the optic such that the {100} plane of the material is on the optic flat, we can calculate the resolved critical stress on the {110} slip plane. The maximum resolved shear stress on the {110} plane will be approximately 0.25 MPa. This is a small value and based on values found in the literature for critical resolved shear stress (see ref. 5) there should be no significant dislocation motion at this shear load.

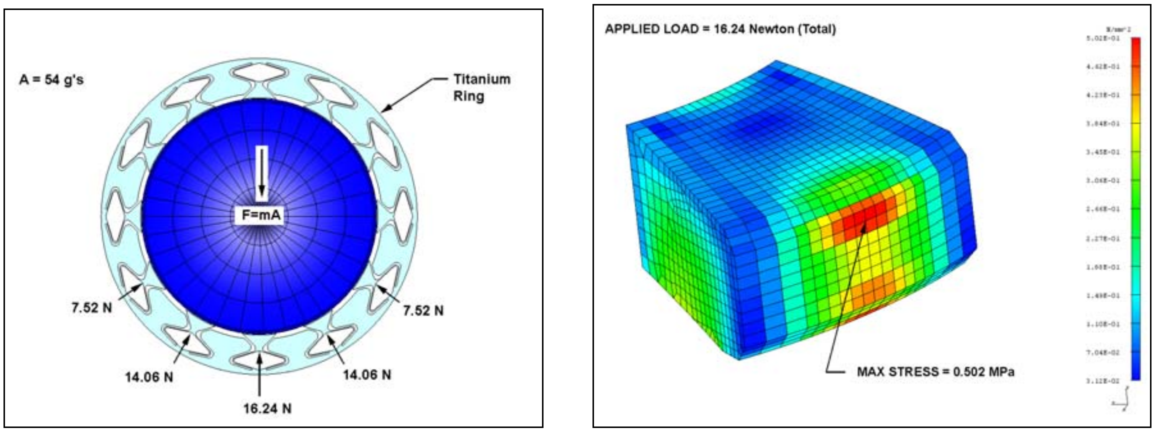

Figure 8 Lithium Fluoride Lens Max Stress due to Applied F = 16.24 Newtons

Flexural stress was also calculated for the Ti-6Al-4V material during the worst case launch load and was found to be well within required safety factors at 263 MPa. (Figure 9)

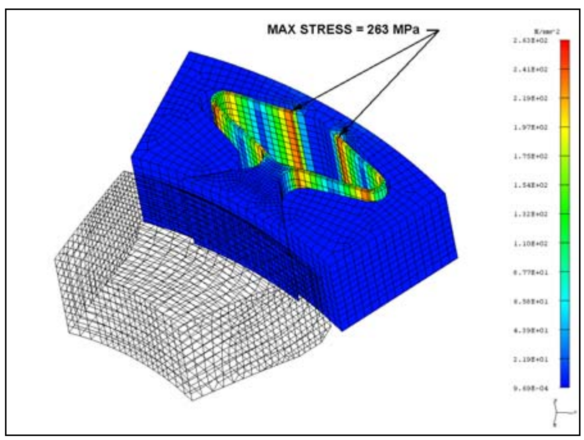

Figure 9 - Titanium Flexure Maximum Stress

Thermal Analysis

The primary thermal concern for this mount was that cooling post launch would cause a significant gradient across the lens and that the lens would fracture as a result. Lithium Fluoride and Barium Fluoride are both very susceptible to thermal shock, so a gradient that was too high would be unfavorable. After discussion with members of the FLITECAM team (ref. 6) our goal was to keep the gradient in the LiF lens below 7K. Thermal analysis and testing suggested that even with a conservative cool down profile, this goal would be easy to reach. In the analysis that was performed, gradients across the lens came in at a maximum of 1K during worst case cool down.

4.0 TESTING RESULTS

Mechanical Vibration – Lens survival

The 12 pad diamond flexure lens mount assembly was tested in vibration to the Qualification spectrum shown in Figure 7 for a duration of 2 minutes.   The fixture shown in Figure 10 was used for vibe. As mentioned earlier, the vibration profile chosen for test is part of the GEVS. Prior to assembling the lens cell, the lens was placed in front of a ZYGO interferometer and its reflective wave front characterized. Once this was done, the lens was placed into the lens mount and bolted to a stiff vibration fixture. Vibration was conducted in all three axes, and accelerometer data for each axis was collected. Once the vibration test was complete, the lens cell was disassembled and the lens re-examed under the ZYGO.

The lens that was vibrated in the 12 pad flexure mount showed virtually no WFE change before and after vibration testing. (See Figure 11)

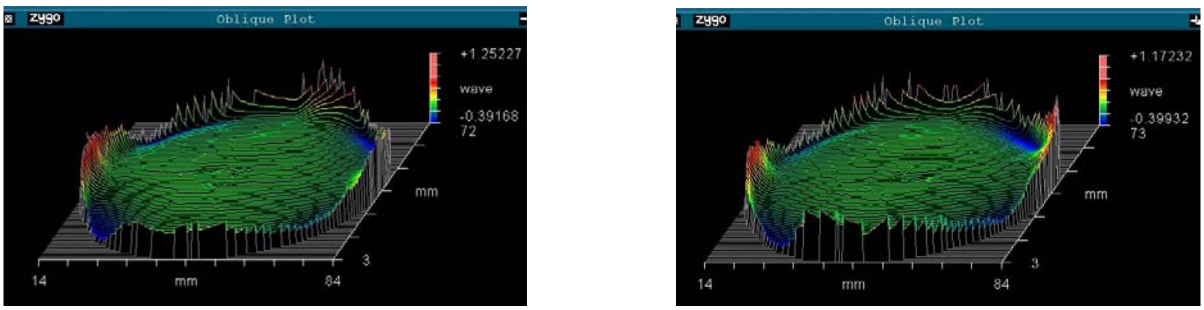

Figure 11 – Comparison of the surface maps for the LiF optic pre and post vibration in the 12 pad diamond flexure mount. The pre-vibe plot is on the right; rms WFE was 0.128 waves, 1.644 waves P-V. The post vibeplot is on the right; rms WFE value was 0.134 waves, 1.572 P-V. Note that the optical quality prior to vibe for this optic was not as good as the optic vibed in the original mount.

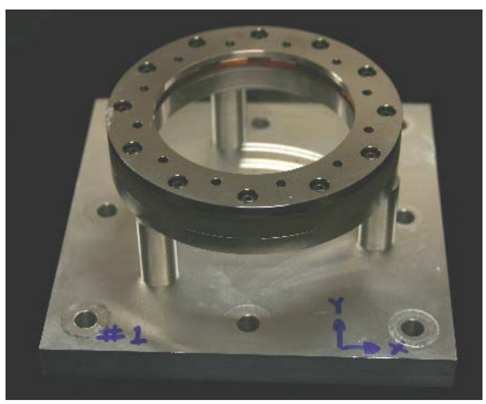

Figure 10 – The test fixture for the 12-pad vibration test

Mechanical Vibration – Lens centration

A test was also conducted to determine how well the mount would maintain lens centration after vibration. For this test, a pair of KAMAN differential sensors was used in conjunction with a dummy aluminum lens. Aluminum has almost the same density as LiF, so it makes an excellent mass simulator for the purposes of test. The dummy lens had a centrally located post on either side with machined flats for the KAMAN sensors to measure. (See figure 10) The KAMAN sensors were bolted to a fixture along with the lens cell. The fixture was then bolted to the vibration test bench. The lens cell and the fixture were assumed to act as a rigid body, so any motion witnessed by the KAMAN sensors should be the result of the lens moving in the cell.

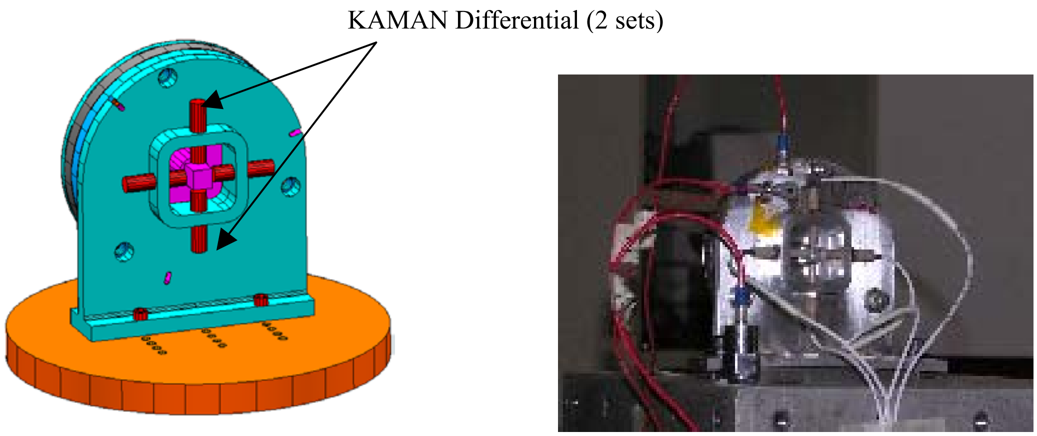

Figure 12 – KAMAN differential sensor set-up with lens dummyand photo of actual set-up

Results of the testing can be seen in Figure 13. Results from two consecutive runs are pictured. The data shown were taken from the X direction accelerometer during a vibration in the X direction. The mount was not disturbed in between the two runs. During the first run, the lens is seen to move ~5 microns in X from beginning to end. During the second run, despite movement during the actual vibe, the difference in position before and after vibe is almost indiscernible. Data for the other axes was similar in nature.

While this is certainly not a statistical set of data (since only one run was conducted for each axis), the conclusion that can be taken from the data is clear. Despite an attempt during assembly to assure that the optic is properly seated in its mount, it takes a vibration cycle to get the optic to truly seat in the mount. Once seated, the centering stability during vibration appears to be excellent. Further optical testing to verify these results in forthcoming.

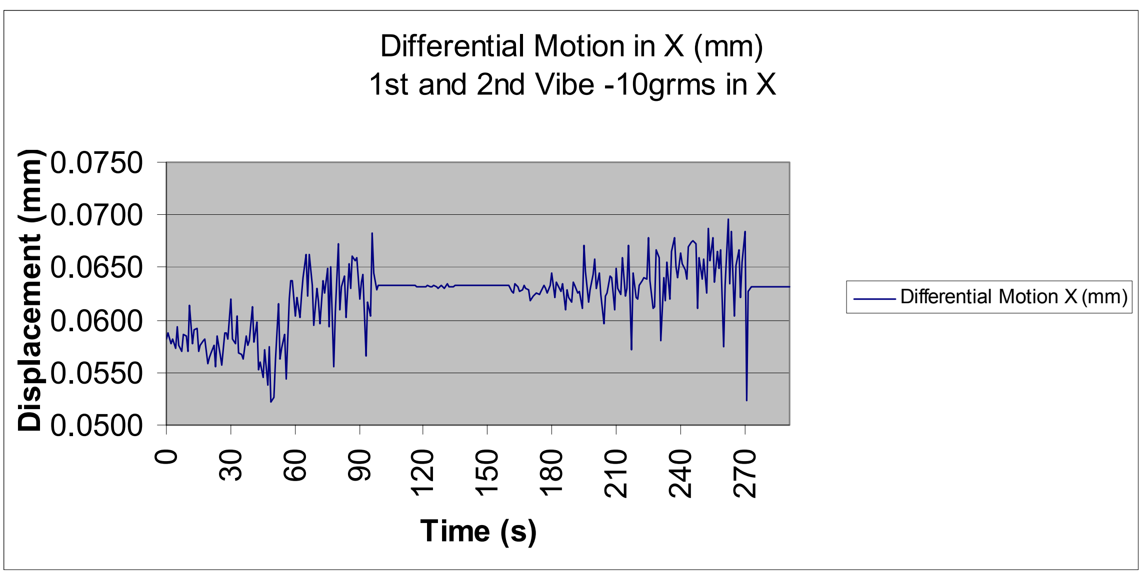

Figure 13 – Decentration results for vibration of the dummy lens cell assembly

Cryogenic cycling – Lens centration

Another key test that we needed to conduct was to test the capability of the mount to keep the optic centered during a cryogenic temperature cycle. In order to accomplish this, the same test set-up that was used in vibration centration testing was used here. The test set-up was bolted to a cold plate in a thermal vacuum chamber and cooled to below 30K. (See figure 14) Several thermo-couples were placed on the test set-up and the lens cell was cooled to 20K. During cool down, gradients between the different areas of the lens cell were measured. Displacement data was also taken from the differential KAMAN sensors. Two cryo-cycles were conducted over the space of two days.

Figure 14 – The centration set-up on the cold plate

Data from the test are presented in Figure 15 and 16. It is important to note that vibe testing did not occur on this reassembled mount prior to cryo-cycling. Had it been conducted, it is likely that the results would have been different, as the first cryo-cycle appears to have had much the same affect as the first vibration run that was discussed above. Both decentration axes are plotted. Decentration was quite high (over 50 microns) in the X-axis during the first cryo-cycle. Note that the slop of the decentration/time plot is highest when the gradient in the system is highest. Once the gradient starts to decrease, the rate and magnitude of decentration goes down as well.

During the second cryo-cycle, the decentration plot looks more stable and does not wander around nearly as much as was the case in the first cycle. Again, while this data cannot in any sense be considered the final word, it points in a direction that makes perfect sense. Cryo-cycling, in addition to vibration appears to help seat the optic into a more stable position. In addition, the motion of the optic in this test appears to be well within the required +/- 50 microns value.

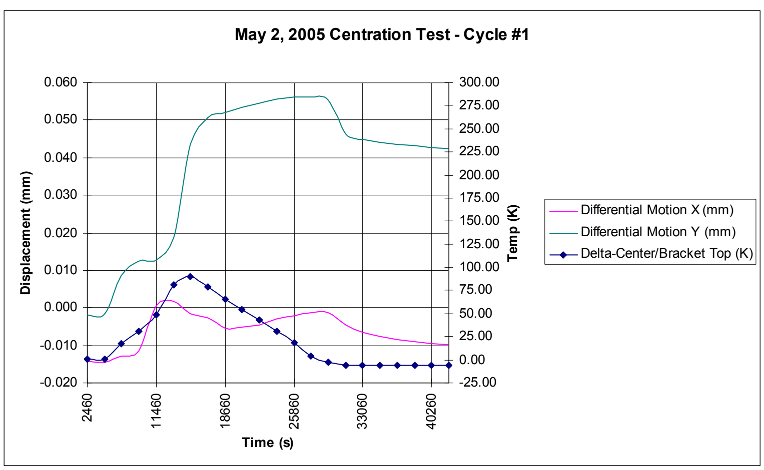

Figure 15 First Cryo-cycle data

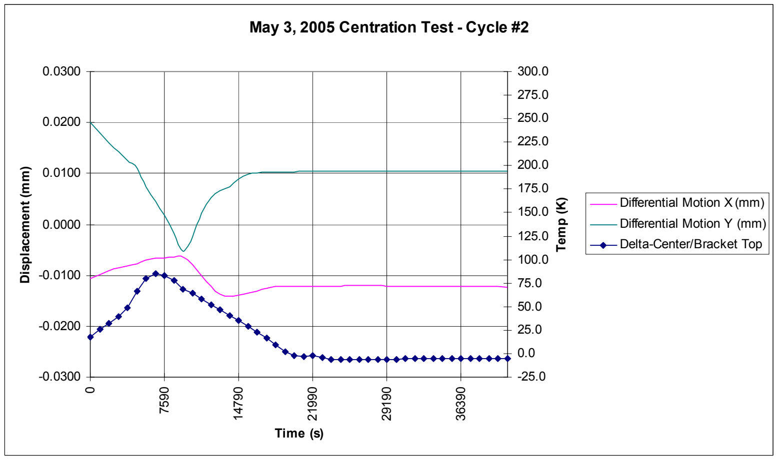

Figure 15 – Second Cryo-cycle data

5.0 CONCLUSION

In this paper we have presented a mount for a 70mm Lithium Fluoride optic intended for use in space at 35K. The mount has been shown to successfully prevent the optic from plastically deforming during vibration and has also been shown to keep the optic centered well within required values during vibration and cryo-cycle. To our knowledge, Lithium Fluoride optics of this size have never before been flown in space for use on board a high performance astronomical instrument. It is our hope that this work will provide new possibilities in the challenging world of infra-red astronomical space systems.

6.0 FUTURE WORK

Several aspects of this work are ongoing. Testing of ETU and flight lens cells for NIRCam (which the work in this paper supports) will be presented at future conferences. Optical methods for determining centration errors during vibration and cool-down will be used for these lens cells and will be directly correlated to system performance.

The authors also continue to work toward a fuller understanding of plasticity in Lithium Fluoride. A vast amount of research has been performed on this material over the pat 60 years as is evidenced by the many papers in the literature. This paper discusses the foundational work that has been done at the Lockheed Martin ATC. We continue to build on this foundation and our understanding of this material continues to grow.

7.0 ACKNOWLEDGMENTS

We would like to thank a number of people who have contributed to the development of this lens mount. Dave Stubbs and Mark Sullivan offered their thoughts early on in the design process and provided suggestions for improvement based on their experience. Jeff Williams and Terri Peters provided valuable expertise in the area of test. Dr. Craig Hom has been instrumental in developing our understanding of Lithium Fluoride. Dr. James Earthman of UC Irvine and Dr. Jerry Wittenauer of Lockheed Martin have also been a tremendous help in understanding the unique materials issues related to single crystal plasticity.

This paper is dedicated to the memory of Aram Mika. His passion for excellence and for his work was infectious.

8.0 REFERENCES

1. Verbal communication, Brad Picarillo, Optical Solutions Incorporated

2. E. Todd Kvamme, Dr. James Earthman, Douglas B. Leviton, “Lithium fluoride material properties as applied on the NIRCam instrument” Proc. SPIE Int. Soc. Opt. Eng. **5904**, (2005) not yet published
3. L.W. Huff “JWST NIRCam Optics” Proc. SPIE Int. Soc. Opt. Eng. **5904**, (2005) not yet published
4. GEVS-SE Rev A, Goddard Space Flight Center, Greenbelt Maryland, June 1996
5. W.G. Johnston, J.J. Gilman, “Dislocation Velocities, Dislocation Densities, and Plastic Flow in Lithium Fluoride”, *Journal of Applied Physics*, Vol. 30, No.2, Feb. 1959
6. Verbal communication, Amy Mainzer, FLITECAM for SOFIA